doi:10.2533/chimia.2021.845 Chimia 75 (2021) 845–855

Recent Approaches towards the Development of Ru(II) Polypyridyl Complexes for Anticancer Photodynamic Therapy

Albert Gandioso,[#] Kallol Purkait,[#] and Gilles Gasser*

Abstract: Photodynamic therapy (PDT) is a remarkable alternative or complementary technique to chemotherapy, radiotherapy or immunotherapy to treat certain forms of cancer. The synergistic effect of light, photosensitizer (PS) and oxygen allows for the treatment of tumours with an extremely high spatio-tumoral control, therefore minimizing the severe side effects usually observed in chemotherapy. The currently employed PDT PSs based on porphyrins have, in some cases, some limitations, which include a low absorbance in the therapeutic window, a low body clearance, photobleaching, among others. In this context, Ru(II) polypyridyl complexes are interesting alternatives. They have low lying excited energy states and the presence of a heavy metal increases the possibility of spin-orbit coupling. Moreover, their photophysical properties are relatively easy to tune and they have very low photobleaching rates. All of these make them attractive candidates for further development as therapeutically suitable PDT PSs. In this review, after having presented this field of research, we discuss the developments made by our group in this field of research since 2017. We notably describe how we tuned the photophysical properties of our complexes from the visible region to the therapeutically suitable red region. This was accompanied by the preparation of PSs with enhanced phototoxicity and high phototoxicity index. We also discuss the use of two-photon excitation to eradicate tumours in nude mice. Furthermore, we describe our approach for the selective delivery of our complexes using targeting agents. Lastly, we report on our very recent synergistic approach to treat cancer using bimetallic Ru(II)-Pt(IV) prodrug candidates.

Keywords: Medicinal inorganic chemistry · Metals in medicine · Photodynamic therapy (PDT) · Photosensitizer · Ru(II) polypyridyl complex

Albert Gandioso was born in Barcelona (Spain). Albert undertook his PhD (2014–2018) in the group of Dr. Vicente Marchán at the University of Barcelona (Spain). The overall goal of his thesis was to develop novel chemical tools for the visualization and treatment of cancer by combining the luminescence properties of coumarins with ligand-targeted delivery strategies. In 2017, he made a 6-month research internship in the group of Dr. Martin Schnermann at the National Cancer Institute (NCI) in US. In 2019, Albert worked as a Postdoctoral Researcher at the Institute for Research in Biomedicine (IRB) in the group of Prof. Modesto Orozco. There, he worked on the optimization and validation of a promising therapeutic RNA tool for combined cancer therapy. He was recently awarded a fellowship from the Association pour la Recherche contre le Cancer (ARC) to work in the group of Gilles Gasser at Chimie ParisTech, PSL University (France).

Kallol Purkait was born and grew up in West Bengal, India. He obtained his Bachelor's and Master's degrees from the University of Calcutta, India. He then moved to the Indian Institute of Science Education and Research Kolkata for his PhD. He completed his PhD on the topic 'Anticancer activity of Palladium & Ruthenium complexes: Effect of steric hindrance on cytotoxicity and GSH resistance' under the supervision of Prof. Arindam Mukherjee. Currently, he is working as a Postdoctoral Researcher in the group of Gilles Gasser at Chimie ParisTech, PSL University (France). His current research focuses on the development of novel light-sensitive prodrugs as anticancer drug candidates.

Born, raised and educated in Neuchâtel, ***Prof. Gilles Gasser*** worked, after his studies, at Lonza (Visp) before moving back to Neuchâtel to obtain his PhD thesis in 2004 with Prof. Helen Stoeckli-Evans. After two post-doctoral stays in the groups of Prof. Leone Spiccia (Monash University, Australia) and Prof. Nils Metzler-Nolte (Ruhr-University Bochum, Germany), Gilles started his independent career at the University of Zurich in 2010, obtaining a Swiss National Science Foundation Assistant Professorship in 2011. In 2016, Gilles moved to Chimie ParisTech, PSL University to take a PSL

*Correspondence: Prof. G. Gasser, E-mail: gilles.gasser@chimieparistech.psl.eu
Chimie ParisTech, PSL University, CNRS, Institute of Chemistry for Life and Health Sciences, Laboratory for Inorganic Chemical Biology, F-75005 Paris, France
#These authors contributed equally.

Chair of Excellence. Gilles was the recipient of several fellowships and awards including the Alfred Werner Award from the Swiss Chemical Society, an ERC Consolidator Grant, the Jucker Award, the European Bioinorganic Chemistry medal and the Pierre Fabre Award for therapeutic innovation from the French Société de Chimie Thérapeutique (SCT).

1. Introduction

The use of light holds enormous potential in anticancer chemotherapy since it offers the possibility of controlling, at a desired time and place, the release of cytotoxic species from an inert prodrug. For this reason, many efforts have been dedicated to the development of novel therapies for improving drug efficacy and, more importantly, to reduce the toxic side-effects associated with the current platinum-based drugs. Photodynamic therapy is an advanced medical technique to treat certain types of tumours. In this strategy, a photosensitizer (PS) harvests light and oxygen to produce reactive oxygen species (ROS), which are responsible for cell killing. The main advantages of this technique over classical chemotherapy are the lowering of side effects due to the very high spatio-temporal activation and less likelihood for drug resistance.[1] Despite its many advantages, this strategy is not suitable for the treatment of metastasised cancers or large hypoxic tumours due to the low concentration of oxygen in the core of large tumours.[2] An ideal PDT PS should have certain criteria, which are i) a very low dark cytotoxicity and high cytotoxicity in the presence of light, ii) the ability to absorb light in the 600–900 nm window to treat deep-seated or large tumours, iii) no production of any toxic metabolites, iv) a selective accumulation in the tumour and targeting of cell organelles to induce cell death, v) a low rate of photobleaching, and vi) favourable pharmacokinetic properties, *i.e.* optimal absorption, distribution, metabolism and excretion (ADME) properties.

The basic mechanism of electron movement between different electronic states upon absorption of light and production of ROS is described in Fig. 1. After initial light absorption, some of the ground state electrons of the PS start to populate their ^{1}ES (singlet excited state) from the ^{1}GS (singlet ground state). Then, the electrons in the excited state can return to the ^{1}GS by radiative (fluorescence) or nonradiative (thermal radiation) decay. In another pathway, excited electrons can go from the ^{1}ES to the ^{3}ES (triplet excited state) through intersystem crossing (ISC) and then returns to the ^{1}GS by radiative (phosphorescence) or nonradiative (relaxation) decay. Of particular interest in view of PDT, a longer triplet excited state lifetime and populated ^{3}ES would be favourable to generate $^1O_2$ in hypoxic conditions for the treatment of hypoxic tumours.[3] The processes of ROS generation are following two pathways, namely Type-1 and Type-2, both are well described in the literature (Fig. 1).[4] The ROS produced are the species responsible for cell killing.

Currently, the most used PSs in the clinics are based on a tetrapyrrolic scaffold (*i.e.* porphyrin, chlorine). However, these families of compounds have, in some cases, some limitations like poor water solubility, photobleaching, low body clearance, low cancer cell selectivity, *etc.*[5] In this context, metal-based photosensitizers are gaining increasing attention due to the very low or almost negligible amount of photobleaching observed,[6] and possible efficient and ultrafast population of triplet excited state due to efficient spin-orbit coupling.[7] Ru(II), Pd(II), Pt(II), Pt(IV), Os(II), Re(I), or Ir(III) complexes have been or are currently being investigated as PDT PSs.[8] In this context, two metal complexes, Photosens® (n = 1–4) and TOOKAD® soluble, have been approved for clinical uses as PDT-PS whereas a few others (Sn complex; Purlytin®, Lu complex; Lutrin®/Antrin®, and Ru complex TLD1433) are in clinical trial (Fig. 2).[8a,9] Among the choice of different metal complexes, ruthenium complexes, especially Ru polypyridyl complexes (RPC) are one of the most studied PSs to treat cancers. In general, a large Stokes shift, efficient ROS production, low photobleaching are the reasons of the choice of RPC. Several strategies have been applied by different groups. Those are mainly 1) change in donor atom from N'-N', to N'-C' or N'-O' to get low lying easily available ES, 2) conjugation with a drug or a biologically active molecule to obtain a synergistic effect and selectivity, 3) bimetallic complex, and 4) a prodrug approach. Moreover, several efforts have been given from different laboratories, including our group, to deliver RPC selectively to the cancer cell by encapsulating inside polymers to form nanoparticles.[10] As a highlight, the first Ru(II) RPC, namely TLD-1433 developed by McFarland and co-workers is currently in Phase-II clinical trial for the treatment of bladder cancer[8a,11] (Fig. 2). Recent findings on RPCs showed important immune modulatory effects,[12] which may have a beneficiary role to suppress cancer.

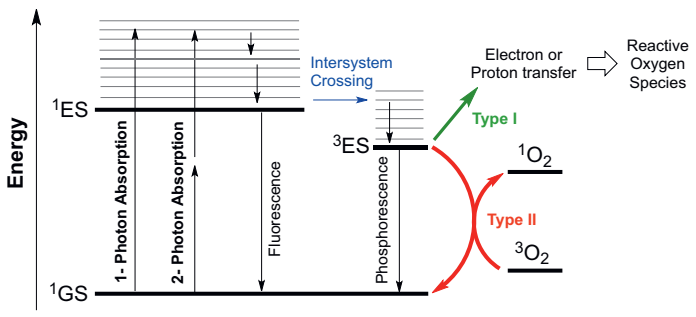

Fig. 1. Photosensitization (one- and two-photon absorption) and mechanism of reactive oxygen species generation.

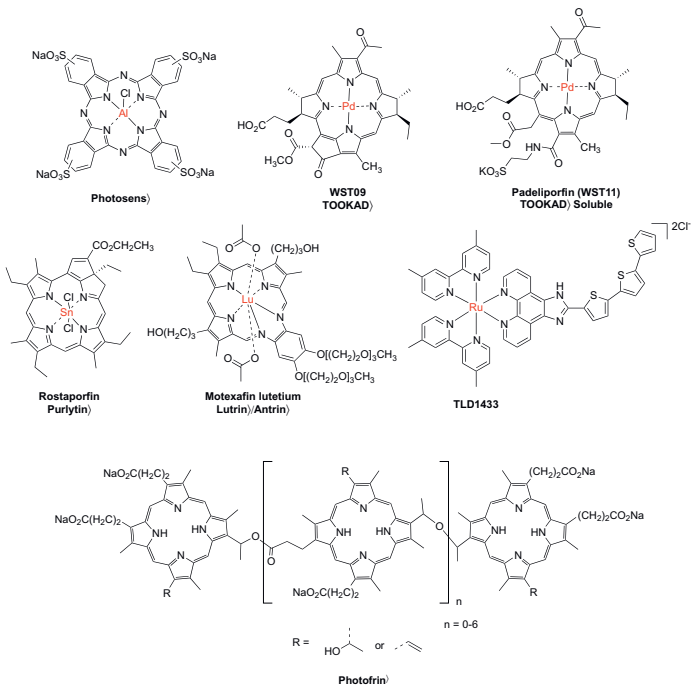

Fig. 2. Metal-based PSs investigated for PDT treatment.

The current PSs used in the clinics to treat cancers are based on one-photon absorption with excitation wavelength range between 400 and 762 nm.[1,13] Importantly, recent developments suggest that two-photon activation could be effectively used to treat tumours that reside 2 cm deep in the body. This distance is considerably bigger than that obtained with one-photon activation.[14] In two-photon absorption, a short laser pulse with very high intensity is used to excite a PS by simultaneous two-photon

absorption. The reason behind the use of a high intensity pulse is to make sure two photons absorb simultaneously. The energy of each photon contributes half of the actual energy for the excitation of an electron. Hence, near-infrared light can be employed to achieve even deeper tissue penetration with minimum biological damage. The process can be quantified in terms of two-photon absorption cross-section (σ2) and expressed in Goeppert-Mayer (GM). In this context, the clinically used PDT PS Photofrin® (Fig. 2) showed a σ2 of 10 GM in methanol at 850 nm.[15] A recent review on this topic showed that, on average, RPCs have a slightly higher σ (160–210 GM).[16] Our lab has recently developed a RPC with a σ2 of *ca.* 6800 GM at 750 nm.[17]

This review highlights some of the achievements of our group in the use of Ru(II) polypyridyl complexes as PDT PSs since 2017, following up on a previous review.[4] More specifically, in this article, we first discuss the development of traditional Ru(II) polypyridyl complexes in combination with different N'-N' ligand systems and their selective delivery using targeting agents. Furthermore, our recent work on bimetallic complexes is also discussed.

2. Novel Ru(II) Polypyridyl Complexes

In continuation of our previous work on PSs having higher wavelength absorption, we prepared a Ru(II) complex of dipyrido[3,2-a:2',3'-c]phenazine (dppz) with either a bpy or phen ligand.[18] Our aim was to evaluate the structure–activity relationship between two complexes (**1** and **2**) (Fig. 3). Unfortunately, poor absorption and emission properties were unveiled for both complexes. We then found that the complexes were non-toxic against tested human cervical cancer cells (HeLa) both in the dark and in the presence of light although the complexes were able to generate $^1O_2$ by harvesting 420 nm light and $^3O_2$.

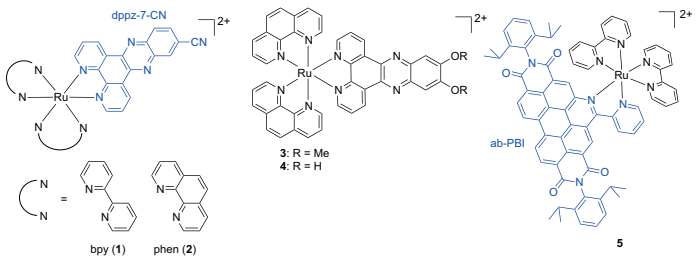

Fig. 3. Chemical structures of Ru(II) complexes (**1–5**) for PDT applications.

In one of our previous works, we found that a 7-methoxy substituted dppz-containing RPC, namely $[Ru(bpy)_2(dppz\text{-}7\text{-}OMe)]^{2+}$, had a good phototoxic index (PI = IC_{50} in the dark/ IC_{50} upon light irradiation) of 42 against HeLa cells upon irradiation with 420 nm light.[19] Therefore, two $[Ru(phen)_2dppz]^{2+}$ derivatives were then prepared with different functional groups on the dppz ligand [dppz-7,8-$(OMe)_2$ (**3**), dppz-7,8-$(OH)_2$ (**4**)] to investigate the effect of small changes of functional group (*i.e.* from methoxy to hydroxy) on the photophysical properties and the phototoxicity of the RPCs (Fig. 3).[20] Very similar absorption spectral properties were obtained for both complexes with a typical metal-to-ligand charge-transfer (MLCT) absorption band in the visible region (400–500 nm) for both complexes **3** and **4**. An intense emission band at 620 nm in acetonitrile solution was observed for both complexes upon excitation at 420 nm. However, the emission intensity was quenched in the presence of water due to the interaction of water with the dppz ligand through H-bonding.[21] The luminescence quantum yield values in acetonitrile for both complexes were comparable (Φ_{em}: 2.8% and 1.7% for complexes **3** and **4**, respectively) with the corresponding parent complex $[Ru(phen)_2(dppz)]^{2+}$ (Φ_{em} = 3.3%). This indicates that the substitution has almost no influence on the excited state. The presence of oxygen had an important influence on the lifetime of the excited state for both complexes **3** and **4**. Hence, we found that the GS of molecular oxygen can interact with the ^{3}ES complexes **3** and **4**. The methoxy-substituted complex (**3**) showed a long luminescence lifetime (aerated: 325 ns and degassed: 645 ns in acetonitrile). Thanks to a collaboration with the Chao group, we could show that both complexes had a much higher two-photon absorption (TPA) cross-section (**3**: 245 GM and **4**: 93 GM at around 800 nm) than the clinically approved PS, H_2TPP (<20 GM at 800 nm).[15] Cellular localization studies suggest that the more lipophilic complex **3** was taken up more by cancer cells than the complex **4** and distributes throughout the cytoplasm and nucleus of HeLa cells. In contrast, the hydroxyl group-containing complex **4** only accumulated in the cell membranes with almost three times less uptake efficacy than **3**. Complex **3** showed dark toxicity against HeLa cells (IC_{50} = 36.5 μM) whereas complex **4** was found to be nontoxic. Interestingly, both complexes showed enhanced toxicities with phototoxic index (PI) values 12 and 6, respectively upon irradiation at 420 nm light. Complex **3** was also found to be active against HeLa cells spheroids with an IC_{50} of 9.5 μM upon exposure of 800 nm light (two photon absorption) with PI value 11.

Würthner and co-workers developed an azabenz-annulated perylene bisimide (ab-PBI) ligand-containing Ru complex (**5**, Fig. 3),[22] which shows a highly populated triplet state with a 4.2 μs lifetime. Moreover, the complex showed absorbance up to 600 nm. All these photophysical properties are basic features for an interesting PS. Therefore, we evaluated the ability of **5** to act as a PDT PS.[23] Complex **5** was found to produce a very low amounts of $^1O_2$. We then evaluated the toxicity of this complex against human ovarian carcinoma (A2780), cisplatin resistant human ovarian carcinoma (A2780R), and HeLa cells. We found that the toxicity slightly increased upon exposure of 420 nm light with PI values of *ca.* 2. We observed that the complex preferentially localized in the nucleus. This was confirmed by ICP-MS measurements.

The low absorbance in the biological therapeutic window is one of the common constraints of RPCs. To target this issue, we functionalized one bpy ligand with aldehyde of the $[Ru(phen)_2(bpy)]^{2+}$ complex **6** (Fig. 4) to have a handle to increase the conjugation.[24] This extended conjugation could decrease the HOMO-LUMO gap, resulting in a lower energy absorption. This derivatization makes the system versatile for further functionalization. Most importantly, upon functionalization with the aldehyde group, complex **6** showed a red-shifted MLCT absorption band with a Stokes shift of 35 nm in comparison to $[Ru(bpy)_3]^{2+}$. Complex **6** can generate high amounts of $^1O_2$ as indicated by the decrease in the fluorescence lifetime in aerated acetonitrile solution. An enhanced phototoxicity (PI = 1.2) of **6** against HeLa cells was observed in the presence of 480 nm light. Importantly, the benzyl amine functionalized complex **7** showed almost 11-fold increase in toxicity towards HeLa cells upon 510 nm light irradiation. In another work with the same aim, namely preparing RPCs that absorb at higher wavelengths, we functionalized the $[Ru(bpy)_3]^{2+}$ core with vinyl dimethylamino groups to give complex **8** (Fig. 4).[25] We could observe a 65 nm red shift of the absorption maximum (515 nm) with an absorption tail up to 650 nm of complex **8** in comparison to the parent complex $[Ru(bpy)_3]^{2+}$. The functionalization also enhanced the molar absorption coefficient. Unfortunately, complex **8** showed poor emission and photostability but a much higher uptake than the parent $[Ru(bpy)_3]^{2+}$ complex. The cytotoxicity of **8** against HeLa cells was found to increase from >200 μM (dark) to 146.3 μM upon 540 nm light irradiation.

2,2':6',2''-terpyridine (terpy) is a ligand that has been widely used in studies related to DNA binding and DNA photo-cleavage activity.[26] For this reason, we used terpy and terpy-functional-

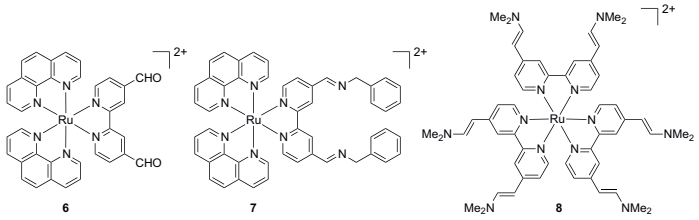

Fig. 4. Chemical structures of Ru(II) complexes **6–8**.

ized ligands in our design to prepare complexes **9–15** (Fig. 5).[27] All the complexes showed a spin-allowed d-π MLCT transition band at 400–550 nm. Importantly, all complexes only slightly photobleached upon constant irradiation with 450 nm light. Complexes **9–14** were found to be non-toxic against HeLa cells both in the presence and absence of light. While complex **15**, which has a dimethylamine functionalization, had an IC_{50} value of *ca.* 35 μM in the dark. This value slightly decreased (PI = 1.4) in the presence of 480 nm light.

From these observations, we concluded that the increase in conjugation and dimethylamine or methoxy functionalization in the bpy or bpy type ligands may have a positive role for red-shifted absorption maxima and phototoxicity.

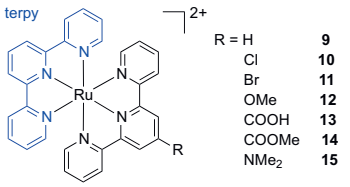

Fig. 5. Chemical structures of Ru(II) complexes **9–15**.

As mentioned before, the majority of currently reported RPC-based PSs typically absorbs in the blue or UV region, which limits their PDT effect on deep-seated or large tumours. Hence, a proper design of complexes that absorb towards higher wavelengths (600–900 nm) is necessary to overcome this drawback. To reach this aim, we have extensively utilized TD-DFT calculations to predict absorption properties in collaboration with the Ciofini group. After calculations, the theoretically-guided lead complexes were synthesized (**16–22**, Fig. 6) in collaboration with the Spingler group.[28] We integrated different modifications on the bpy ligand before coordinating the resulting ligands to $[Ru(phen)_2Cl_2]^{2+}$ and $[Ru(bphen)_2Cl_2]^{2+}$ ((phen = 1,10-phenanthroline) and (bphen = 4,7-diphenyl-1,10-phenanthroline)) (Fig. 6). In particular, we synthesized the (*E*,*E*')-4,4'-bis(N,N'-dimethylaminovinyl)-2,2'-bipyridine ligand (highlighted in blue, Fig. 6). The corresponding complexes **20** and **22** showed the desired red-shift maximum absorption (λ_{max}). Importantly, the red-shift in absorption spectra of these complexes are well aligned with the theoretical predictions of HOMO-LUMO gap. We believe that this theoretically guided design approach will definitely increase the possibility to design PDT PSs in the future. Importantly, biological studies revealed that complexes **16–20** and **22** were found to be nontoxic in the dark ($IC_{50,\ dark}$ > 100 μM) in mouse colon carcinoma (CT-26), human glioblastoma (U87), human glioblastoma astrocytoma (U373), HeLa, and noncancerous retina pigmented epithelial (RPE-1) cells. Upon irradiation (480 nm, 10 min, 3.21 $J.cm^{-2}$), the complexes based on a $[Ru\text{-}(phen)_2(bpy)]^{2+}$ scaffold (**16–20**) presented poor phototoxicity (IC_{50}: >100–52.54 μM). In contrast, the compounds based on the $[Ru(bphen)_2(bpy)]^{2+}$ scaffold (**21** and **22**) showed a notable phototoxicity upon light irradiation (IC_{50}: 15.21–0.19 μM). This effect can be attributed to the significantly higher cellular uptake of the compounds, as determined by ICP-MS. Notably, complex **21** showed a PI around 23.5 against CT-26 cells ($IC_{50,\ 595\ nm}$; 60 nM) upon exposure to 595 nm light. This complex was found to be stable in human plasma as well as upon light irradiation, which is a prime criterion for a PS. It localized in the cytoplasm of HeLa cells as determined by confocal microscopy. Based on these results, we performed additional biological experiments to demonstrate the potential of these novel compounds upon irradiation with red light (595 nm). For this purpose, the Seahorse XF instrument was used as it allows for real time measurements of oxygen consumption rate (OCR) and extracellular acidification rate (ECAR) in cells. Also, we performed additional and important assays, specifically, 3D multicellular tumour spheroids (MCTS) growth inhibition assay. MCTSs simulate the conditions found in clinically treated tumours including hypoxia and proliferation gradients. So, irradiation at 595 nm led to the disturbance of mitochondrial respiration and glycolysis processes in HeLa 2D monolayer cells (Fig. 7) as well as 3D multicellular tumour spheroids (MCTSs). Overall, these techniques presented here can be applied for the synthesis of other metal complexes as PDT agents.

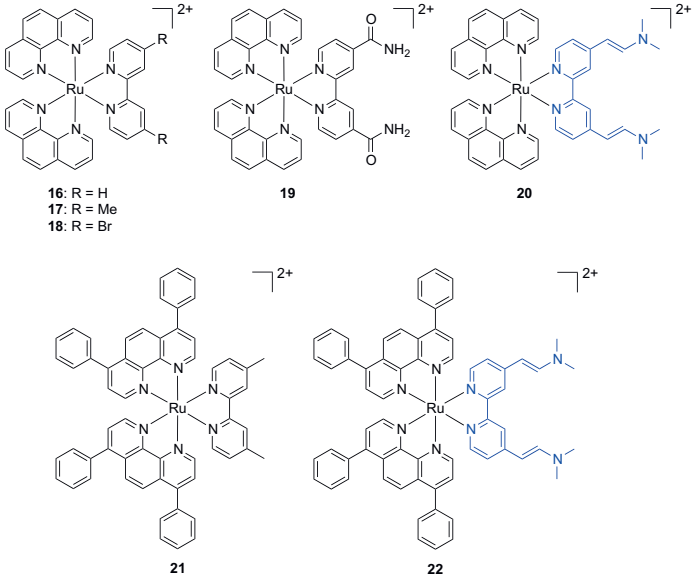

Fig. 6. Chemical structures of ruthenium (II) complexes investigated by our group (**16–22**). The part of complex **20** and **22** highlighted in blue indicates the ligand (*E*,*E*')-4,4'-bis(N,N'-dimethylaminovinyl)-2,2'-bipyridine.

Based on these results, we further utilized this *in silico*-based design approach to obtain a red-shifted absorption. More specifically, we used an extended π-conjugation along with dimethyl amine or a methoxy group attached to the bpy as bidentate ligand.[17] We envisioned the introduction of donor groups to shift the absorption maxima in the biological relevant therapeutic window. Theoretical calculations predicted two bands (MLCT/LMCT and ligand-centred (LC) charge-transfer excitations) in the 400–600 nm region. Furthermore, most detailed theoretical ground and excited state property studies indicate that the most intense lowest lying 2P absorption processes are associated with LCCT transitions. Overall, theoretical studies predicted both 1P and a strong 2P absorption probability of the corresponding Ru(II) complexes. We therefore synthesized three new ligands: i) (*E*,*E*')-4,4'-bisstyryl-2,2'-bipyridine (Fig. 8A), ii) (*E*,*E*')-4,4'-bis[p-(N',N'-dimethylamino)styryl]-2,2'-bipyridine (Fig. 8B) and iii) (*E*,*E*')-4,4'-bis[p-methoxystyryl]-2,2'-bipyridine (Fig. 8C).[17] After obtaining the corresponding complexes (**23–29**) shown

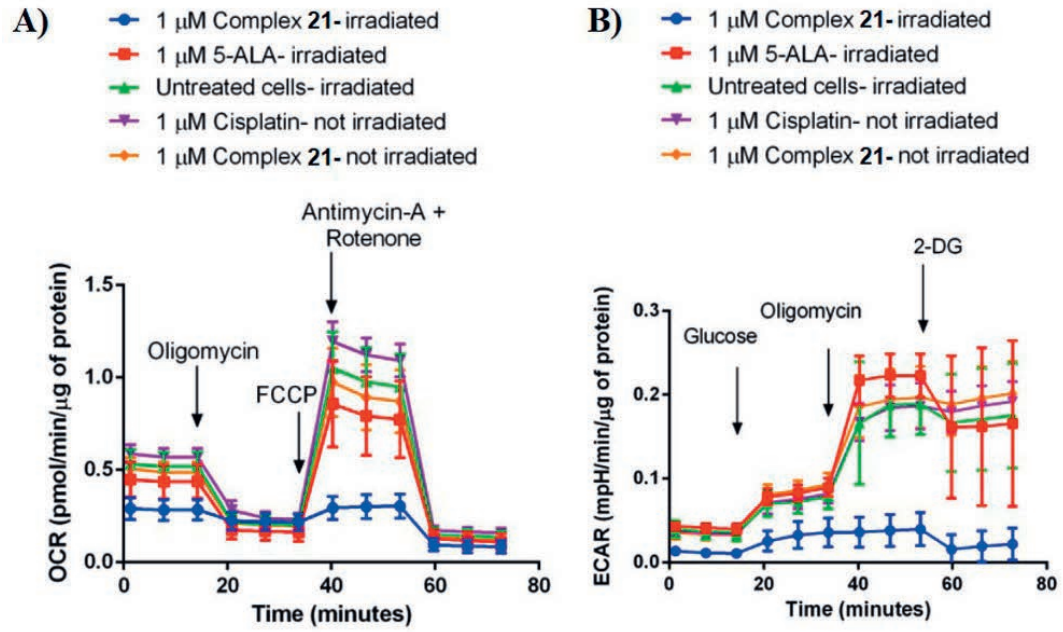

Fig. 7. A) Oxygen consumption rates and different respiration parameters in CT-26 cells alone or after treatment with **21**. B) Extracellular acidification rates and different glycolysis parameters in CT-26 cells alone or after treatment with **21**. Reproduced with permission from. ref. [28]. Copyright © 2020, American Chemical Society

in Fig. 8D, the photophysical studies revealed that their λ_{max} was red-shifted by around 50–70 nm compared with [Ru(2,2'-bipyridine)$_3$]$^{2+}$. Also, the compounds presented an exceptionally strong two-photon (2P) absorption with values up to ~6800 GM. The theoretical predictions match well for both the 1P and 2P absorption properties. The complexes with the methoxy groups (**24**, **26** and **29**) presented impressive singlet oxygen quantum yields (52%, 54% and 75%, respectively) in acetonitrile. Importantly, all compounds were found to be stable in human plasma at 37 ºC for 48 h in the dark as well as photostable. Also, the cellular localization studies by both confocal microscopy and quantifying the Ru concentration in different organelles by ICP-MS indicate their preferential accumulation in the cytoplasm. All complexes were found to be nontoxic in the dark (IC_{50} = > 100 μM) in RPE-1 cells (noncancerous), HeLa, CT-26, and U373 cell lines. Phototoxicity studies under irradiation at 480 nm and 540 nm showed that the complexes were toxic in the micromolar range: $IC_{50,\ 480\ nm}$ = 0.7–53.6 μM, and $IC_{50,\ 540\ nm}$ = 0.9–83.1 μM. The most cytotoxic complex **24** showed $IC_{50,\ dark}$ > 100 μM, $IC_{50,\ 480\ nm}$ = 0.7 ± 0.4 μM, $IC_{50,\ 540\ nm}$ = 0.9 ± 0.3 μM against CT-26 cells with a great PI value > 143. Cell death mechanism studies showed that the complexes follow either an apoptosis or both an apoptosis and para-apoptosis pathway. In view of these good preliminary results, we investigated their cytotoxic effects on 3D MCTS. Confocal microscopy studies indicated the relatively quick uptake of asymmetric complexes (**23**–**26**) to the inside core of MCTS, whereas symmetric complexes (**27**–**29**) were mostly found on the outer surface of MCTS. However, upon incubation for a longer time, it was internalized to the inside core. In dark conditions, spheroids show an asymptotic growth of complex-treated 3D HeLa MCTS, that confirms the non-toxic effect without irradiation. But, upon 1P light (500 nm) or 2P light (800 nm), 3D spheroids treated with **23**–**26** were completely eradicated. Strikingly, complex **24** is nontoxic up to 300 μM against 3D MCTS and highly phototoxic in the low micromolar range ($IC_{50,\ 800\ nm}$ > 1.4 ± 0.2) with PI values of 250 (Fig. 9). One of the most relevant studies of this work are the *in vivo* experiments. In collaboration with the Chao group, we chose a multiresistant doxorubicin-selected P-gp-overexpressing human colon cancer tumour model (SW620/AD300) that is very difficult to treat. Compound **24** was injected intravenously to tumour-bearing mice (2 mg/kg). While tumours of mice treated with **24** in the dark kept growing, after one PDT procedure (irradiation at 1P (500 nm, 60 min) or 2P irradiation (800 nm, 50mW, 1 kHz)), tumour size significantly decreased, as shown in Fig. 10. Importantly, after the treatment, we did not find any significant pathological effect to the organs, as observed in H&E staining. Overall, these results provide valuable insights for the design and optimization of Ru(II) complexes for PDT. This theoretically guided development has been recently highlighted.[29]

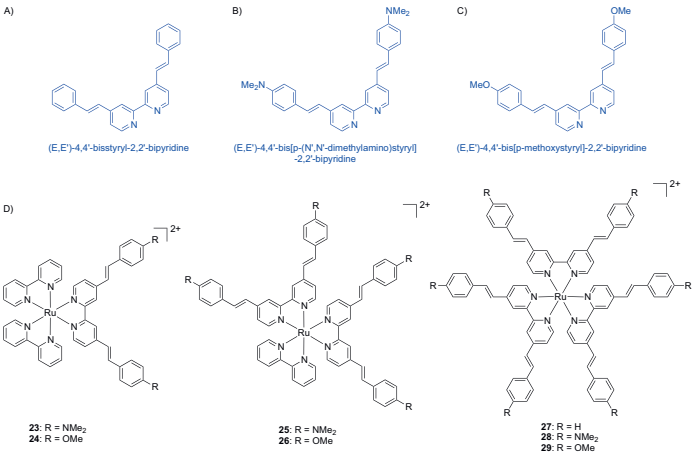

Fig. 8. A) – C) Chemical structures of bpy derivatives used to synthesize complexes **23**–**29**, and D) chemical structures of RCPs investigated as 1P and 2P PDT PSs (**23**–**29**).

In another work, we modified the DNA intercalating ligand dppz to synthesize a novel family of complexes (**30**–**34**, Fig. 11) due to the interesting results obtained with other dppz-based complexes for the production of $^1O_2$, internalization and phototoxicity values.[19,30] More specifically, we explored the derivatization of the dppz ligand with halogen groups (F, Cl, Br, and I) to increase the lipophilicity of the complexes, therefore increasing membrane permeability. We studied different parameters of the new series of compounds, such as generation of singlet oxygen, UV-Vis absorption, Log*P* and photocytotoxicity. The λ_{max} bands were similar to the previously reported ruthenium polypyridyl dppz complexes (350–400 nm).[19] The broad band centred at 450 nm (MLCT transition) did not seem to be affected by the incorporation of the halogen groups. The octanol/water partition coefficient (Log*P*)

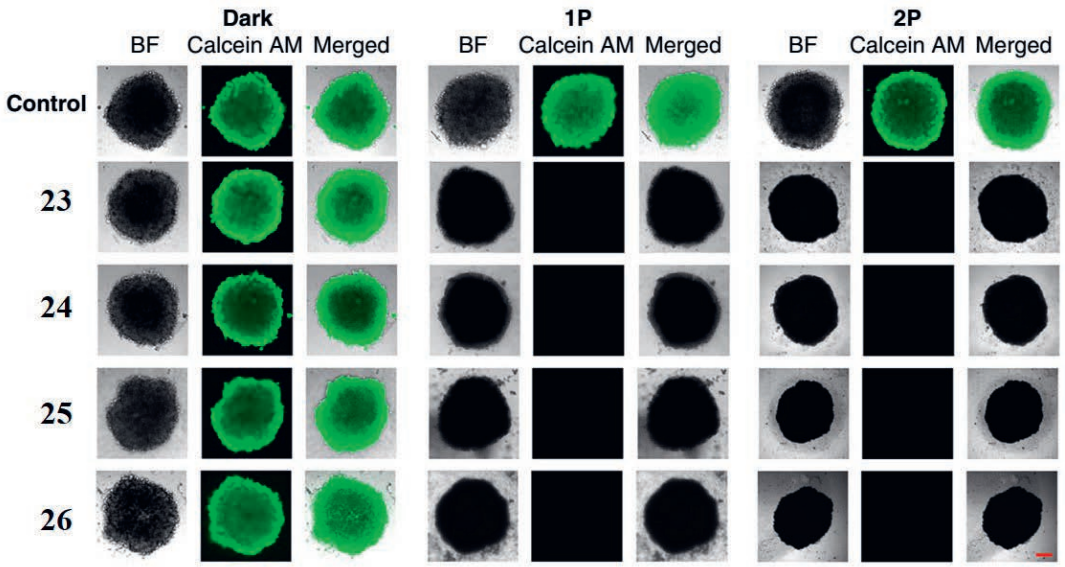

Fig. 9. Representative image of the cell viability assay in 3D-HeLa MCTS. MCTS were treated with compounds **23–26** (20 µM, 2% DMSO, v%) in the dark for 3 days. After this time, MCTS were kept in the dark, exposed to 1P irradiation (500 nm, 16.7 min, 10.0 mW.cm^{-2}, and 10 J.cm^{-2}) or 2P irradiation (800 nm, 10 J.cm^{-2}, and section interval of 5 µm). After 2 days, the cell viability was assessed by measurement of the fluorescence of calcein (λ_{ex} = 495 nm, λ_{em} = 515 nm), which is generated in living cells from Calcein AM. The scale bar represents a length of 200 µm.[17] Copyright © 2020, The Author(s).

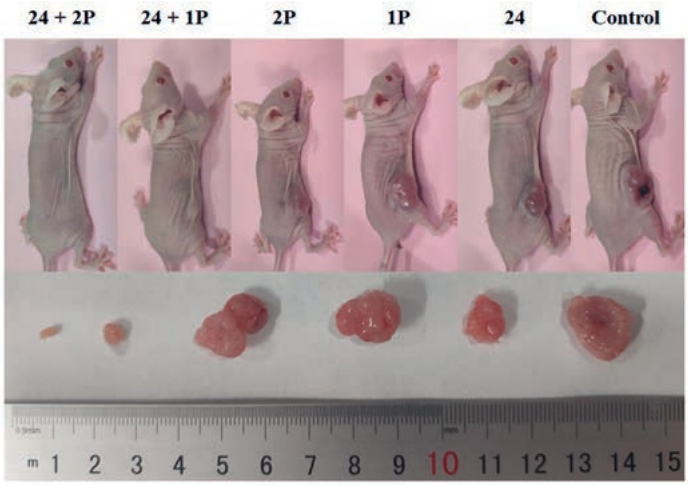

Fig. 10. *In vivo* PDT study of **24** using 1P (500 nm, 60 min, 10.0 mW.cm^{-2}, and 36 J.cm^{-2}) or 2P (800 nm, 50 mW, 1 kHz, pulse width 35 fs, and 5 s.mm^{-1}) excitation on nude mice bearing a doxorubicin-selected P-gp-overexpressing human colon cancer tumour (SW620/AD300). Representative photographs of the tumour-bearing mice.[17] Copyright © 2020, The Author(s).

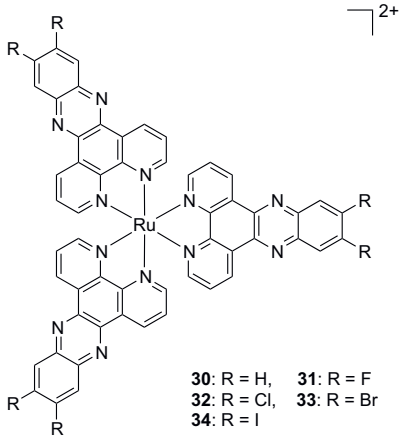

Fig. 11. Chemical structures of RPCs investigated as PDT PSs (**30–34**).

is an important parameter that gives some hints on the ability of a compound to passively diffuse into cells. Log*P* determination revealed that the lipophilicity of the complexes increased by the introduction of halogen groups to the dppz ligand (H<F<Cl<Br<I). However, counter-intuitively, the phototoxicity of these complexes decreased (PI at 420 nm: *ca.* 47 to *ca.* 1 for complexes **30–34** respectively against HeLa cells) as their lipophilicity increased; this could be explained by the atomic radius of the halogen substituents. Indeed, the intercalation process requires the dppz ligand to get through the DNA's double helix, which could be prevented by the bulky halogen atoms.

3. Bioconjugation of Ruthenium

As mentioned before, RPCs are attractive PSs for PDT. However, they generally present a low selectivity for cancer cells over non-cancerous cells. Therefore, undesired phototoxic effects on a healthy cell can be observed, although the physician is only applying light at a selected area.[1,31] To overcome this limitation, there is a need for the development of a suitable drug delivery system to increase the amount of PS delivered to the tumour. In this context, there is a strong interest of our group towards the design and development of complexes conjugated to small molecules, peptides, antibodies or proteins, *etc.* for i) target selectivity,[32] ii) key enzyme or protein inhibition,[16b,33] or iii) organelle selectivity.[34] This approach increases the specificity and potency of the anticancer agents. In this context, our group is actively involved in utilizing different pathways to achieve more tumour specific uptake. Recently, we described two different strategies: i) specific vitamin receptors and ii) use of nanobody in conjugation with our target complex.

Vitamin B12 is a critical nutrient mainly involved in cell growth and proliferation.[35] The transporter protein, transcobalamin (TC) is responsible for transporting vitamin B12 (Cobalamine: Cbl) from blood to cells. Furthermore, vitamin B12-loaded transcobalamin can be recognized by a specific receptor protein, CD320, present on the cell surface.[36] This receptor is overexpressed in several malignancies including breast, prostate, cervical, colorectal cancer, *etc*.[37] In this context, to tackle this drawback, in collaboration with the Zobi group, we have tagged our complex to vitamin B12 (cobalamine) (Fig. 12).[38] This improved the aqueous solubility of the complexes. The photophysical properties have been compared between Cbl-conjugated and non-conjugated complexes. We found that the ^{3}MLCT band centred at 450 nm in parent complexes has not changed upon Cbl conjugation. Overall, the conjugation had no effect on the photophysical properties of the complexes. Complex **35** showed a very low emission, whereas complex **36** showed an emission maximum at 635 nm upon excitation at 450 nm. For complex **36**, the excited state lifetime

drastically decreases in the presence of $^3O_2$, indicating their interaction. The cytotoxicity of the complexes was evaluated against HeLa cells and non-cancerous RPE-1 cells both in the dark and in the presence of light. We observed that only the parent complex **35** is toxic against both cancerous and non-cancerous cells. Unexpectedly, we lost the toxicities upon conjugation with Cbl both in the dark and upon light irradiation. We conclude that the transcobalamin pathway was not involved in the uptake of our complex.

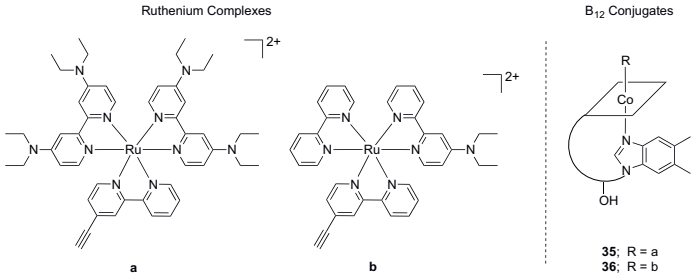

Fig. 12. Chemical structure of complexes **35**–**36**.

In this context, another strategy to increase uptake into tumour cells over healthy cells is the use of fragments of antibody or nanobody (NBs). The use of NBs presents some advantages thanks to their small size, stability, solubility, fast pharmacokinetics, specificity, and affinity for their cognate antigens. Our group recently explored the conjugation of NB to Ru(II) polypyridyl complexes for selective PDT in collaboration with the Zarschler and Stephan groups.[39] We choose the 7C12 NB, known for specific binding to epidermal growth factor receptor (EGFR) expressing cells. EGFR is an important target as it is overexpressed in some solid tumours, such as head and neck, breast, non-small-cell lung, and pancreatic cancer. As shown in Fig. 13, we conjugated $[Ru(phen)_2(dppz)]^{2+}$ to the nanobody, which is known to have excellent phototoxicity. Also, we used a peptide chain with a poly-glycine unit, which is necessary for an efficient and site-specific conjugation. Importantly, the photophysical characterization revealed that all major bands are still comparable between the Ru(II) complex and the NB-Ru(II). One of the essential things in the conjugation of PDT agents is that the photophysical properties are not affected. To demonstrate the receptor-specific uptake, EGFR-positive (A431) and EGFR negative (MDA-MB-435S) cells were incubated for different periods (4, 24, and 48 h) with various concentrations of the bioconjugate in the dark at 37 ºC. The amount of cell-associated ruthenium was determined by ICP-MS. Importantly, the accumulation of **37** after 48 h incubation in A431 cell lines (32.87 ± 4.87 ng/mg protein) was higher if compared with the MDA-MB-435S cell line (5.45 ± 1.32 ng/mg protein). This indicates that the NB conjugation positively affects the intracellular accumulation of the Ru(II) polypyridyl complex. Also, we performed confocal fluorescence microscopy experiments. Notably, NB-Ru(II) showed a predominant membrane staining even after 48 h of incubation at 37 ºC, and only very little intracellular fluorescence was observed. It confirms the site-specific biding of the NB-Ru(II) to the EGPR receptor. Unfortunately, in contrast to expectations, conjugate **37** was found not to produce reactive oxygen species (ROS) in cancer cells and is therefore not phototoxic ($IC_{50,\ dark}$ >25 μM, $IC_{50,\ 480\ nm}$ >25 μM).

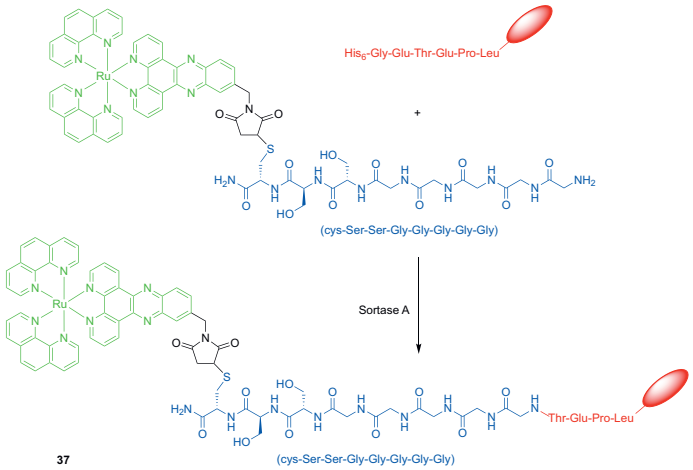

Fig. 13. Overview of the Sortase A-mediated site-specific modification of the NB derivative 7C12-Strep-Sortag-His6 with the $Ru(phen)_2(dppz$-7-maleimidemethyl-S-Cys-$(Ser)_2(Gly)_5$-$NH_2)$ complex resulting in Ru-NB conjugate. The $[Ru(phen)_2(dppz)]^{2+}$ complex is highlighted in green, while the engineered NB is drawn in red and the peptide chain with a poly-glycine unit is depicted in blue. PDB entry of Sortase A from Staphylococcus aureus: 1T2P.[39] Copyright © 2019 The Authors. Published by Wiley-VCH Verlag GmbH & Co. KGaA.

4. Encapsulation of Ru Polypyridyl Complexes for Selective Delivery

In the previous section, we discussed how we utilized receptor-mediated uptake to achieve selectivity of our previously developed promising Ru complexes. At the same time, we are trying to use a potential delivery vehicle to deliver our complex specifically to the cancer cells. More precisely, in this effort, we utilized i) a FDA-approved polymer with terminal biotin and folate group to form nanoparticles, and ii) functionalized silica nanoparticles for selective delivery to the cancer cells.

Previously, we found that complex **38** (Fig. 14) did not have any photocytotoxicity despite ideal photophysical properties for PDT applications. This was found to be due to a low cellular uptake.[19] In collaboration with the Thomas group, we reported the polymeric encapsulation of **38** to polylactide (PLA) (**39**) (Fig. 14).[32a] PLA is a well-established, FDA-approved, biodegradable, biocompatible, and aliphatic polyester for drug delivery applications. To synthesize the covalently bound Ru-containing polymer, we used a ring-opening polymerization (ROP) technique with a biologically friendly Zn initiator instead of commonly used toxic Sn-based initiators. We characterized the nanoconjugate by NMR, MALDI-TOF MS and dynamic light scattering (DLS). Polymers of different molecular weights were synthesized from D,L-lactide, L-lactide, and D-lactide. We then prepared nanoparticles of different size. The influence of molecular weight, tacticity, and nanostructure of the complex loaded polymer on the phototherapeutic activity, cellular uptake, and photosensitizer release kinetics was evaluated. The absorption and emission spectra did not show much difference between the bioconjugate **39** in comparison to **38**. ICP-MS experiments revealed that the conjugate with the higher chain length and hence hydrophobicity accumulated the

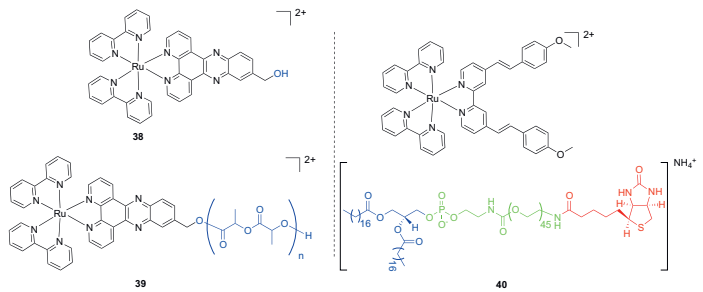

Fig. 14. Chemical structures of conjugates based on RPCs for selective PDT agents. The hydrophilic (blue) and lipophilic (green) parts as well as biotin (red) are marked in colour.

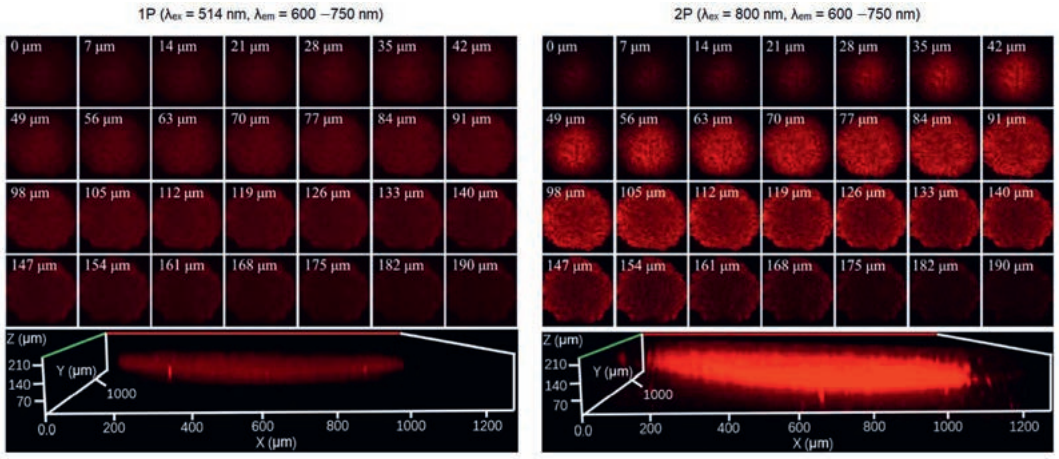

Fig. 15. 1P (λ_{ex} = 514 nm, λ_{em} = 600–750 nm) and 2P (λ_{ex} = 800 nm, λ_{em} = 600–750 nm) excited Z-stack images after incubation of NP (4.95 µM) for 12 h in a 500–600 µm cancerous adenocarcinomic human alveolar basal epithelial (A549) MCTS (Above). (Below) Z-axis images scanning from the top to the bottom of an intact spheroid every 7 µm, 3D Z-stack of an intact spheroid.[40] Copyright © 2020, American Chemical Society.

most into the cells. In agreement with the uptake experiments, photocytotoxicity studies revealed that this conjugate had, upon light irradiation at 480 nm, an IC_{50} value of 4.4 µM after 48 h incubation in HeLa cells. Overall, this work demonstrates how to tackle poorly cellular uptake to transform a non-photo toxic PS to an active PS for PDT in a controlled fashion.

Following our earlier report on complex **24**,[17] we have found a way to increase tumour selectivity by utilizing a FDA-approved PEGylated phospholipid polymer. To do so, we functionalized this polymer with biotin (vitamin B7) before complex encapsulation (**40**) (Fig. 14).[40] In this context, it is important to mention that due to a high proliferation rate, cancer cells have an unregulated vitamin uptake receptor (sodium multivitamin transporter (SMVT)), over the cell surface. Due to abnormal growth and arrangement, tumours have also a leaky vascular system. The vasculature of the tumour is markedly disorganized and twisted in comparison to the vasculature of normal cells. Vascular endothelium in tumours proliferate rapidly and discontinuously, resulting in a greater number of open fenestrations and unions than in normal vessels. Therefore, the EPR effect permits the accumulation of molecules of certain size (typically liposomes, nanoparticles, and macromolecular drugs) in tumour tissues much more than they do in normal tissues. Hence, we targeted both SMVT and the permeability and retention effect (EPR)-mediated uptake to deliver our complex.

Importantly, upon encapsulation, the luminescence quantum yield ($\Phi_{em,\,38}$ = 0.9%, $\Phi_{em,\,NP}$ = 3.1%) in water increases drastically and even little more than observed in acetonitrile ($\Phi_{em,\,38}$ = 2.8%). Further confocal microscopic studies indicated their selective accumulation inside the lysosome, which is further confirmed by the quantification of Ru in lysosome by ICP-MS experiments. The cellular uptake studies with different inhibitors and the complex revealed that the complex is used mainly in the SMVT mediated uptake and the endocytosis pathway. Strikingly, we also observed that NP uptake was around 20 times higher in SMVT overexpressed A549 cells in comparison to noncancerous human lung fibroblasts (HLF) cells. The NPs showed much less toxicity in the dark (IC_{50} > 494.7 µM) against all of our tested cells but the toxicity increased upon light exposure (IC_{50}, 1P = 3.2–3.6 µM, IC_{50}, 2P = 3.2–3.5 µM) with PI, >139 – >155. Our complex-encapsulated NP is also cytotoxic against cisplatin-resistant A549 cells and a higher decrease in cytotoxicity was observed against noncancerous HLF cells (IC_{50}, 1P = 48.1 µM, IC_{50}, 2P = 48.2 µM). The NPs can activate caspase-3/7 and follow the apoptosis pathway for cell killing. From confocal microscopy studies, we observed the accumulation of the Ru complex inside the core of spheroids (Fig. 15). The NPs showed low micromolar 1P and 2P phototoxicity against MCTS with PI >108.7 and >113.6 respectively. In addition, during *in vivo* studies, using the same amount of the Ru(II) polypyridine complex, the particles were found to accumulate 8.7 times more inside the tumour than the complex alone, demonstrating its cancer-targeting effect. Upon light exposure at clinically relevant 1P (500 nm) or 2P (800 nm) excitation, the nanoparticles were found to have a high phototoxic effect of eradicating a tumour inside a mouse model (Fig. 16) with no pathological alteration of organ tissue.

Based on the promising results of complex **40**, we further explored the potential of this type of delivery system with the analogous polymer with terminal folic acid groups. Folate receptors (FRs), which are involved in the uptake of folic acid, exist in three different isoforms (α, β, and γ). Among them, FRα is expressed at very low levels in healthy cells. Still, it is highly up-regulated on the cell surface of a wide variety of cancer cells, including ovarian, kidney, brain, triple-negative breast and colon cancer. Therefore, it is a well-established target for selectively deliver PDT agents. With this in mind, our group prepared folate-targeted Ru(II) nanoparticles.[41] More specifically, we described the en-

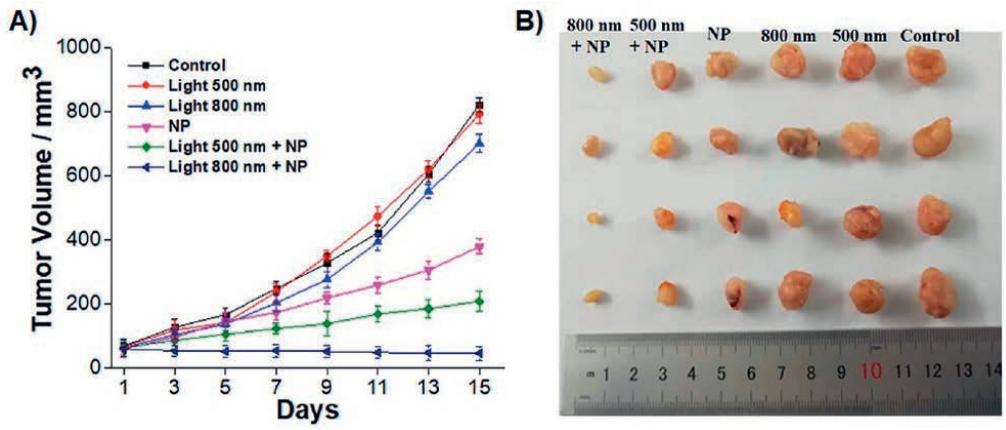

Fig. 16. *In vivo* PDT study of A549-bearing nude mice. (A) Tumour growth inhibition curves upon 1P (500 nm, 10 mW/cm^2, 60 min) or 2P (800 nm, 50 mW, 1 kHz, pulse width of 35 fs, 5 s/mm) treatment. (B) Representative photographs of tumours harvested 15 days after the treatment.[40] Copyright © 2020, American Chemical Society.

capsulation of [Ru(phen)$_2$(4,4'-dimethyl-2,2'-bipyridine)]$^{2+}$ into DSPE-PEG$_{2000}$-folate (**41**, Fig 17). Importantly, upon encapsulation, the absorption and emission spectra of nanoparticles **41** were found to be similar to the Ru(II) polypyridyl complex itself. Having established the photophysical properties of nanoparticles **41**, we focused on investigating photocytotoxicity towards cancerous human ovarian carcinoma (A2780) and its corresponding cisplatin resistant (A2780 CIS) and doxorubicin resistant (A2780 ADR) cell lines. It is well-known that these cell lines overexpressed the FRα (0.8 pmol/mg) contrary to the noncancerous human normal lung fibroblast (MRC-5) cells, which have a level of the FRα in the normal range (0.6 pmol/mg). While the Ru complex showed toxicity in the dark in the micromolar range (IC_{50} = 4.17–9.53 μM), the corresponding nanoformulation NPs did not show any toxicity in the dark (IC_{50} > 100 μM). This work clearly demonstrates that the encapsulation of the Ru(II) polypyridyl complex (**21**) may drastically decrease undesired dark toxicity. Upon irradiation at 480 or 595 nm, a phototoxic effect in the micromolar range for Ru (IC_{50} = 0.27–0.72 μM) and NPs (IC_{50} = 2.64–63.8 μM) with high phototoxic indices (PI) for NP of up to >37.9 μM was determined. Notably, the nanoparticles were found to have a significantly higher phototoxicity in the ovarian cancer cell lines (IC_{50} = 2.64–3.92 μM), which overexpresses the folate receptor, compared to the lung fibroblast cell line (IC_{50} = 40.51–63.83 μM), which has a normal level of the folate receptors, suggesting a folate targeting effect. The selective accumulation of the Ru(II) complex into the cancer cells was determined by ICP-MS. The uptake of NPs (25 μM, 4 h) in A2780 was higher, 8-times more, in comparison with the value in MRC-5 cells. Following these promising biological experiments, we explored the use of these novel NPs in 3D multicellular tumour spheroids (MCTS). Promisingly, the nanoparticles did not have a cytotoxic effect in the dark. Irradiation with red-light engendered phototoxicity in the lower micromolar range ($IC_{50,595\ nm}$ = 9.62 ± 0.93 μM, PI > 10.4). Overall, these results indicate that the NPs are able to penetrate a 3D MCTS and to act as a PDT PS at 595 nm.

Very recently, our group, in collaboration with the team of Gómez-Ruiz described the attachment of Ru(II) polypyridyl complexes into mesoporous silica nanoparticles (MSNs).[42] This type of particle presents some advantages compared to the standard nanoparticles like their lower price and synthetic accessibility. For this purpose, we derivatized the MSNs with folic acid to increase the selectivity for cancer cells over healthy cells. As mentioned before, the folic acid receptor is overexpressed in different cancer cells. Therefore, we synthesized complexes **42** and **43** (Fig. 18), analogues of [Ru(bphen)$_2$(4,4'-dimethyl-2,2'-bipyridine)]. The photophysical properties of the Ru(II) polypyridine complexes and corresponding conjugates (MSNs and MSNs-FA) are in the same range as the previously reported compound **21**.[28] Importantly, the observed lifetimes strongly decreased in the presence of air, suggesting that molecular oxygen ($^3O_2$) can interact with the excited state of the Ru(II) polypyridine complex to generate singlet oxygen ($^1O_2$). All silica nanoparticles were found to be nontoxic in the dark in the tested cell lines. The potential targeting of folate receptor overexpressing cancer cells was evaluated by comparison

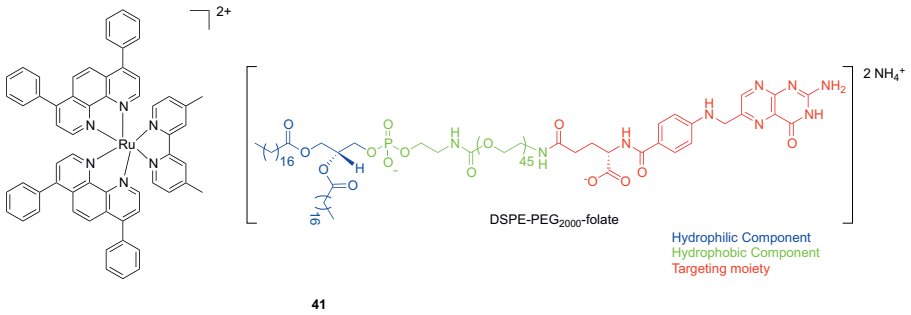

Fig. 17. Chemical structures of the Ru(II) polypyridine complex and polymers used for nanoparticle formulations. The hydrophilic (blue) and lipophilic (green) parts as well as folate (red) are marked in colour.[41]

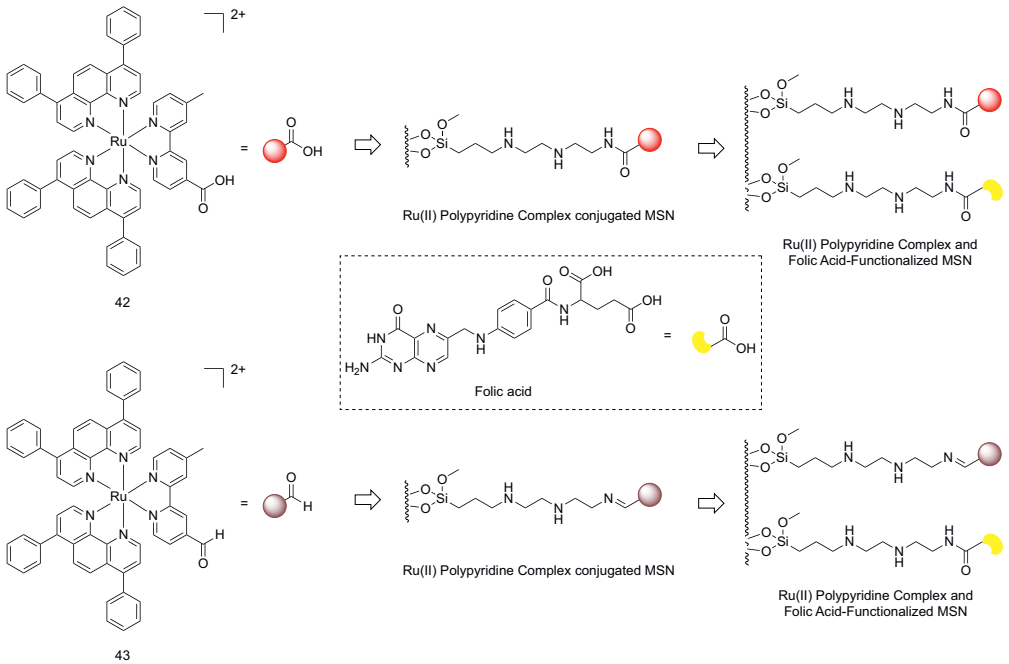

Fig. 18. Chemical structures of complexes **42** and **43**, and synthesis of the Ru(II) polypyridine complex and folic acid-functionalized mesoporous silica nanoparticles.

of the cytotoxicity between noncancerous human normal lung fibroblast (MRC5) cells, which have folate receptors in the normal range, with cancerous human ovarian carcinoma (A2780) cells, which are well-known to have an overexpressed number of folate receptors. The particles without attached FA caused a phototoxic effect upon irradiation at 480 or 540 nm in the low nanomolar range without differentiating between cancerous and noncancerous cells. On the contrary, the MSNs with FA upon irradiation at 540 nm showed interesting IC_{50} values (> 500 μg/mL; > 133–360 nM) in MRC5. In contrast, the A2780 showed IC_{50} in the lower nanomolar range, according to the overexpression of the folate receptor. ($IC_{50,\ 480\ nm}$ = 43–159 μg/mL; 31–42 nM and $IC_{50,\ 540\ nm}$ = 61-187 μg/mL; 44–50 nM).

5. Heterometallic Ruthenium (II)–Platinum(IV) Complexes

Platinum(II)-based drugs are widely used in chemotherapy to treat almost all types of cancer.[43] The main target of these drugs is DNA: they bind to DNA, which eventually stops DNA synthesis.[43] The first Pt(II) complex to be approved by the FDA, namely cisplatin (Fig. 19A), showed numerous serious side effects due to its kinetic lability.[44] Therefore, the next generation of anticancer platinum (II) drugs, Carboplatin and Oxaliplatin (Fig. 19A), contain a bidentate oxo-ligand to impart kinetic inertness in the bloodstream. Also, some side effects have been reduced. In this context, octahedral Pt(IV) complexes are kinetically much more inert than Pt(II) complexes. At present, there is a growing interest in the development of Pt(IV) anticancer agents because of the inertness of the low-spin d6 Pt(IV) centre to ligand substitution reactions. This minimizes undesired side-reactions with biomolecules prior to DNA binding. The Pt(IV) complexes used in anticancer research are usually composed of six ligands: two are classified as non-leaving groups, two as leaving groups (such as in conventional Pt(II) complexes), and two extra ligands which occupy the two axial positions (Fig. 19B). These two additional positions offer the possibility of modifying the lipophilicity and solubility of the complex, as well as facilitate the attachment of targeting ligands. The structures of four relevant examples of Pt(IV) complexes (Ormaplatin, Iproplatin, Satraplatin and LA-12.) are shown in Fig 19B. Pt(IV) complexes behave as pro-drugs. They are activated upon reduction from Pt(IV) to Pt(II) by cellular reducing agents like glutathione, ascorbic acid, *etc*. After the first activation, the second activation process is similar to other Pt(II) complexes, *i.e.* by aquation and further binding to DNA to stop replication. Importantly, *trans*,*cis*,*cis*-bis(acetate) amminecyclohexylaminedichlorido platinum(IV) (Satraplatin) was the first platinum agent reported to have oral activity, which was accomplished by improving lipophilicity and stability. In preclinical studies, Satraplatin showed a better toxicity profile than cisplatin, including in cisplatin-resistant human tumour cell lines, like the other Pt(IV) complexes that we mentioned before.

In collaboration with the Gibson group, we developed a novel Pt(IV)–Ru(II) bimetallic complex (**44**), which combines a Ru-based PDT PS and classical chemotherapy based on Pt(IV) (Fig. 19C).[45] In our case, the axial ligands including the Ru(II) complex and phenylbutyrate are released after Pt(IV) reduction. Phenylbutyrate is an important adjuvant anticancer drug.[45] We evaluated the photophysical properties of the Ru(II) and Ru(II)-Pt(IV) complexes. The absorption and emission spectra of the Ru(II) and Ru(II)-Pt(IV) complexes were relatively similar (abs: 438 and 462 nm, em: 623 nm, respectively). As expected, biological studies revealed differences between the Ru(II) and the Ru(II)-Pt(IV) complexes. The IC_{50} values of **44** against HeLa cells upon light irradiation at 595 nm were lower compared to the Ru(II) complex ($IC_{50,\ dark}$: 13.56 μM and 3.26 μM, $IC_{50,\ 480nm}$: 1.65 μM and 0.31 μM and $IC_{50,\ 595nm}$: 0.58 μM and 0.13 μM, Ru(II) and Ru(II)-Pt(IV), respectively). Similar values were obtained on different cell lines, RPE-1 and A2780.

Interestingly, complex **44** showed a much higher phototoxicity activity with IC_{50} values in the nanomolar range. These values are lower than similar types of Ru-Pt bimetallic complexes[46] or the heterometallic Ru(II)-Pt(II) developed by the Zhou group.[47] As a comparison, their reported bimetallic complex (containing four Pt-centres and two Ru-centres) had IC_{50} = 3.3 μM against HeLa cells upon exposure to 450 nm light[47] whereas complex **44** had had IC_{50} = 130 nM against HeLa cells upon exposure of 595 nm light.

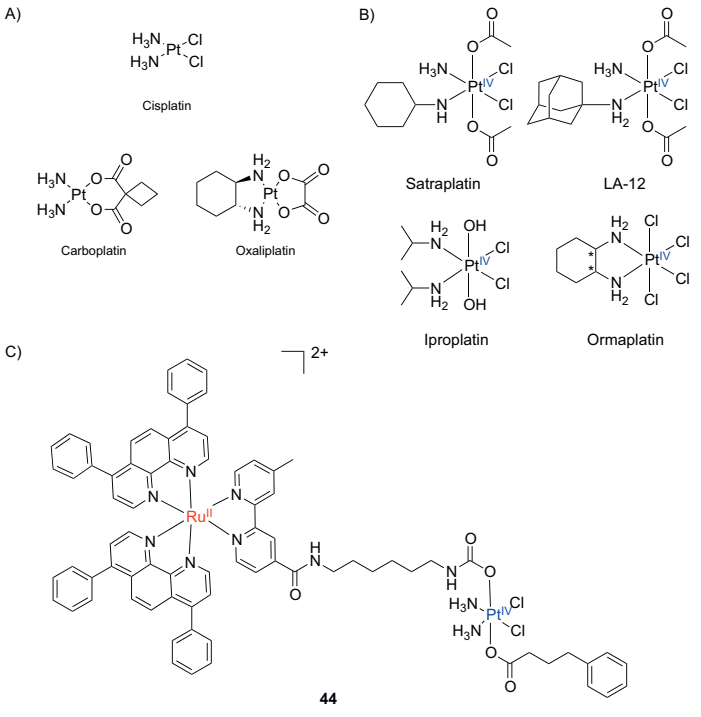

Fig. 19. A) Clinically approved platinum drugs to treat cancers, B) Most relevant examples of Pt(IV) pro-drug and C) Chemical structures of a heterometallic Ru(II)–Pt(IV) complex, **44**.

6. Conclusion

Ru(II) polypyridyl complexes are effective photosensitizers for PDT because of their ability to produce ROS upon visible light absorption and their easily tunable photophysical properties. In recent years, important efforts were made by our group to develop more suitable photosensitizers for therapeutic uses. Hence, in this review, we have discussed our current advancements, highlighting the most important achievements over the last 4 years.

For example, we have successfully introduced a series of new phototoxic (500–800 nm) RPCs based on a theoretical TD-DFT guided designing method. Strikingly, one of these complexes can eradicate tumours completely upon excitation at 595 nm (1P-PDT) and 800 nm (2P-PDT). Nevertheless, these complexes are non-selective for cancer cells. Therefore, we are currently actively trying to achieve selectivity by attaching bioactive molecules to our complexes or by encapsulating them into polymers. As a highlight, we encapsulated the complex into a biotin-containing polymer, allowing for its higher accumulation in tumours xenographted in mice.

Acknowledgements

This work was financially supported by an ERC Consolidator Grant PhotoMedMet to G.G. (GA 681679), by the ITMO Cancer AVIESAN (Alliance Nationale pour les Sciences de la Vie et de la Sante/ National Alliance for Life Sciences & Health) within the framework of the Cancer Plan (G.G) and has received support under the program "Investissements d' Avenir" launched by the French Government and implemented by the ANR with the reference ANR-10-IDEX-0001-02 PSL (G.G.). A.G. thanks the Association pour la Recherche contre le Cancer (ARC) for funding his post-doctoral stay at Chimie ParisTech, PSL University. We

would like to take the opportunity to thank all our colleagues, who have collaborated on the projects discussed in this review article.

Received: June 22, 2021

[1] P. Agostinis, K. Berg, A. Cengel Keith, H. Foster Thomas, W. Girotti Albert, O. Gollnick Sandra, M. Hahn Stephen, R. Hamblin Michael, A. Juzeniene, D. Kessel, M. Korbelik, J. Moan, P. Mroz, D. Nowis, J. Piette, C. Wilson Brian, J. Golab, *CA Cancer J. Clin.* **2011**, *61*, 250, https://doi.org/10.3322/caac.20114.

[2] L. Larue, B. Myrzakhmetov, A. Ben-Mihoub, A. Moussaron, N. Thomas, P. Arnoux, F. Baros, R. Vanderesse, S. Acherar, C. Frochot, *Pharmaceuticals* **2019**, *12*, 163, https://doi.org/10.3390/ph12040163.

[3] R. Lincoln, L. Kohler, S. Monro, H. Yin, M. Stephenson, R. Zong, A. Chouai, C. Dorsey, R. Hennigar, R. P. Thummel, S. A. McFarland, *J. Am. Chem. Soc.* **2013**, *135*, 17161, https://doi.org/10.1021/ja408426z.

[4] F. Heinemann, J. Karges, G. Gasser, *Acc. Chem. Res.* **2017**, *50*, 2727, https://doi.org/10.1021/acs.accounts.7b00180.

[5] a) A. E. O'Connor, W. M. Gallagher, A. T. Byrne, *Photochem. Photobiol.* **2009**, *85*, 1053, https://doi.org/10.1111/j.1751-1097.2009.00585.x; b) M. Ascencio, P. Collinet, M. O. Farine, S. Mordon, *Lasers Surg. Med.* **2008**, *40*, 332, https://doi.org/10.1002/lsm.20629.

[6] a) S. Lazic, P. Kaspler, G. Shi, S. Monro, T. Sainuddin, S. Forward, K. Kasimova, R. Hennigar, A. Mandel, S. McFarland, L. Lilge, *Photochem. Photobiol*. **2017**, *93*, 1248, https://doi.org/10.1111/php.12767; b) E. Yang, J. R. Diers, Y.-Y. Huang, M. R. Hamblin, J. S. Lindsey, D. F. Bocian, D. Holten, *Photochem. Photobiol.* **2013**, *89*, 605, https://doi.org/10.1111/php.12021.

[7] I. C. Lu, C. N. Tsai, Y.-T. Lin, S.-Y. Hung, V. P. S. Chao, C.-W. Yin, D.-W. Luo, H.-Y. Chen, J. F. Endicott, Y. J. Chen, *J. Phys. Chem. A* **2021**, *125*, 903, https://doi.org/10.1021/acs.jpca.0c05910.

[8] a) S. A. McFarland, A. Mandel, R. Dumoulin-White, G. Gasser, *Curr. Opin. Chem. Biol.* **2020**, *56*, 23, https://doi.org/10.1016/j.cbpa.2019.10.004; b) J. Li, T. Chen, *Coord. Chem. Rev*. **2020**, *418*, 213355, https://doi.org/10.1016/j.ccr.2020.213355.

[9] X. Li, B.-D. Zheng, X.-H. Peng, S.-Z. Li, J.-W. Ying, Y. Zhao, J.-D. Huang, J. Yoon, *Coord. Chem. Rev*. **2019**, *379*, 147, https://doi.org/10.1016/j.ccr.2017.08.003

[10] a) N. Soliman, G. Gasser, C. M. Thomas, *Adv. Mater.* **2020**, *32*, 2003294, https://doi.org/10.1002/adma.202003294; b) E. Villemin, Y. C. Ong, C. M. Thomas, G. Gasser, *Nat. Rev. Chem*. **2019**, *3*, 261, https://doi.org/10.1038/s41570-019-0088-0.

[11] https://clinicaltrials.gov/ct2/show/NCT03945162?term=TLD1433&draw=2&rank=2.

[12] F. Ayaz, *Inflammation* **2019**, *42*, 1383, https://doi.org/10.1007/s10753-019-00999-y.

[13] a) M. Nguyen, S. S. Sandhu, R. K. Sivamani, *Clin., Cosmet. Invest. Dermatol.* **2019**, *12*, 427, https://doi.org/10.2147/CCID.S167498; b) C.-N. Lee, R. Hsu, H. Chen, T.-W. Wong, *Molecules* **2020**, *25*, 5195, https://doi.org/10.3390/molecules25215195.

[14] J. R. Starkey, A. K. Rebane, M. A. Drobizhev, F. Meng, A. Gong, A. Elliott, K. McInnerney, C. W. Spangler, *Clin. Cancer Res*. **2008**, *14*, 6564, https://doi.org/10.1158/1078-0432.CCR-07-4162.

[15] A. Karotki, M. Khurana, J. R. Lepock, B. C. Wilson, *Photochem. Photobiol.* **2006**, *82*, 443, https://doi.org/10.1562/2005-08-24-RA-657.

[16] a) L. Zeng, S. Kuang, G. Li, C. Jin, L. Ji, H. Chao, *Chem. Commun.* **2017**, *53*, 1977, https://doi.org/10.1039/C6CC10330H; b) X. Zhao, M. Li, W. Sun, J. Fan, J. Du, X. Peng, *Chem. Commun.* **2018**, *54*, 7038, https://doi.org/10.1039/C8CC03786H.

[17] J. Karges, S. Kuang, F. Maschietto, O. Blacque, I. Ciofini, H. Chao, G. Gasser, *Nat. Commun.* **2020**, *11*, 3262, https://doi.org/10.1038/s41467-020-16993-0.

[18] C. Mari, R. Rubbiani, G. Gasser, *Inorg. Chim. Acta* **2017**, *454*, 21, https://doi.org/10.1016/j.ica.2015.10.010.

[19] C. Mari, V. Pierroz, R. Rubbiani, M. Patra, J. Hess, B. Spingler, L. Oehninger, J. Schur, I. Ott, L. Salassa, S. Ferrari, G. Gasser, *Chem. - Eur. J.* **2014**, *20*, 14421, https://doi.org/10.1002/chem.201402796.

[20] J. Hess, H. Huang, A. Kaiser, V. Pierroz, O. Blacque, H. Chao, G. Gasser, *Chem. - Eur. J.* **2017**, *23*, 9888, https://doi.org/10.1002/chem.201701392.

[21] A. A. Cullen, C. Long, M. T. Pryce, *J. Photochem. Photobiol., A* **2021**, *410*, 113169, https://doi.org/10.1016/j.jphotochem.2021.113169.

[22] M. Schulze, A. Steffen, F. Wuerthner, *Angew. Chem., Int. Ed.* **2015**, *54*, 1570, https://doi.org/10.1002/anie.201410437.

[23] C. Mari, H. Huang, R. Rubbiani, M. Schulze, F. Wuerthner, H. Chao, G. Gasser, *Eur. J. Inorg. Chem.* **2017**, 1745, https://doi.org/10.1002/ejic.201600516.

[24] J. Karges, F. Heinemann, F. Maschietto, M. Patra, O. Blacque, I. Ciofini, B. Spingler, G. Gasser, *Bioorg. Med. Chem.* **2019**, *27*, 2666, https://doi.org/10.1016/j.bmc.2019.05.011.

[25] J. Karges, O. Blacque, P. Goldner, H. Chao, G. Gasser, *Eur. J. Inorg. Chem.* **2019**, *2019*, 3704, https://doi.org/10.1002/ejic.201900569.

[26] a) N. Grover, N. Gupta, P. Singh, H. H. Thorp, *Inorg. Chem.* **1992**, *31*, 2014, https://doi.org/10.1021/ic00037a008; b) B. T. Farrer, H. H. Thorp, *Inorg. Chem.* **2000**, *39*, 44, https://doi.org/10.1021/ic990833u; c) N. Grover, H. H. Thorp, *J. Am. Chem. Soc.* **1991**, *113*, 7030, https://doi.org/10.1021/ja00018a048; d) G. A. Neyhart, N. Grover, S. R. Smith, W. A. Kalsbeck, T. A. Fairley, M. Cory, H. H. Thorp, *J. Am. Chem. Soc.* **1993**, *115*, 4423, https://doi.org/10.1021/ja00064a001; e) A. Jain, C. Slebodnick, B. S. J. Winkel, K. J. Brewer, *J. Inorg. Biochem.* **2008**, *102*, 1854, https://doi.org/10.1016/j.jinorgbio.2008.06.004.

[27] J. Karges, O. Blacque, M. Jakubaszek, B. Goud, P. Goldner, G. Gasser, *J. Inorg. Biochem.* **2019**, *198*, 110752, https://doi.org/10.1016/j.jinorgbio.2019.110752.

[28] J. Karges, F. Heinemann, M. Jakubaszek, F. Maschietto, C. Subecz, M. Dotou, R. Vinck, O. Blacque, M. Tharaud, B. Goud, E. Vinuelas Zahinos, B. Spingler, I. Ciofini, G. Gasser, *J. Am. Chem. Soc.* **2020**, *142*, 6578, https://doi.org/10.1021/jacs.9b13620.

[29] S. Banerjee, *ChemBioChem* **2021**, Ahead of Print, https://doi.org/10.1002/cbic.202100102.

[30] S. Roy, E. Colombo, R. Vinck, C. Mari, R. Rubbiani, M. Patra, G. Gasser, *ChemBioChem* **2020**, *21*, 2966, https://doi.org/10.1002/cbic.202000289..

[31] L. Zeng, P. Gupta, Y. Chen, E. Wang, L. Ji, H. Chao, Z.-S. Chen, *Chem. Soc. Rev.* **2017**, *46*, 5771, https://doi.org/10.1039/C7CS00195A..

[32] a) N. Soliman, L. K. McKenzie, J. Karges, E. Bertrand, M. Tharaud, M. Jakubaszek, V. Guerineau, B. Goud, M. Hollenstein, G. Gasser, C. M. Thomas, *Chem. Sci.* **2020**, *11*, 2657, https://doi.org/10.1039/C9SC05976H; b) Z. Zhao, K. Qiu, J. Liu, X. Hao, J. Wang, *Chem. Commun.* **2020**, *56*, 12542, https://doi.org/10.1039/D0CC04943C; c) E. Du, X. Hu, S. Roy, P. Wang, K. Deasy, T. Mochizuki, Y. Zhang, *Chem. Commun.* **2017**, *53*, 6033, https://doi.org/10.1039/C7CC03337K; d) J.-X. Zhang, M. Pan, C.-Y. Su, *J. Mater. Chem. B* **2017**, *5*, 4623, https://doi.org/10.1039/C7TB00702G.

[33] a) L. N. Lameijer, D. Ernst, S. L. Hopkins, M. S. Meijer, S. H. C. Askes, S. E. Le Devedec, S. Bonnet, *Angew. Chem., Int. Ed*. **2017**, *56*, 11549, https://doi.org/10.1002/anie.201703890; b) K. Arora, M. Herroon, M. H. Al-Afyouni, N. P. Toupin, T. N. Rohrabaugh, L. M. Loftus, I. Podgorski, C. Turro, J. J. Kodanko, *J. Am. Chem. Soc.* **2018**, *140*, 14367, https://doi.org/10.1021/jacs.8b08853.

[34] J. Liu, X. Liao, K. Xiong, S. Kuang, C. Jin, L. Ji, H. Chao, *Chem. Commun.* **2020**, *56*, 5839, https://doi.org/10.1039/D0CC01148G.

[35] M. J. Nielsen, M. R. Rasmussen, C. B. F. Andersen, E. Nexo, S. K. Moestrup, *Nat. Rev. Gastroenterol. Hepatol.* **2012**, *9*, 345, https://doi.org/10.1038/nrgastro.2012.76.

[36] E. V. Quadros, J. M. Sequeira, *Biochimie* **2013**, *95*, 1008, https://doi.org/10.1016/j.biochi.2013.02.004.

[37] A. M. Sysel, V. E. Valli, R. B. Nagle, J. A. Bauer, *Anticancer Res.* **2013**, *33*, 4203.

[38] M. Jakubaszek, J. Rossier, J. Karges, J. Delasoie, B. Goud, G. Gasser, F. Zobi, *Helv. Chim. Acta* **2019**, *102*, e1900104, https://doi.org/10.1002/hlca.201900104.

[39] J. Karges, M. Jakubaszek, C. Mari, K. Zarschler, B. Goud, H. Stephan, G. Gasser, *ChemBioChem* **2020**, *21*, 531, https://doi.org/10.1002/cbic.201900419.

[40] J. Karges, J. Li, L. Zeng, H. Chao, G. Gasser, *ACS Appl. Mater. Interfaces* **2020**, *12*, 54433, https://doi.org/10.1021/acsami.0c16119.

[41] J. Karges, M. Tharaud, G. Gasser, *J. Med. Chem.* **2021**, *64*, 4612, https://doi.org/10.1021/acs.jmedchem.0c02006.

[42] J. Karges, D. Diaz-Garcia, S. Prashar, S. Gomez-Ruiz, G. Gasser, *ACS Appl. Bio Mater.* **2021**, *4*, 4394, https://doi.org/10.1021/acsabm.1c00151.

[43] D. M. Cheff, M. D. Hall, *J. Med. Chem.* **2017**, *60*, 4517, https://doi.org/10.1021/acs.jmedchem.6b01351.

[44] T. C. Johnstone, K. Suntharalingam, S. J. Lippard, *Chem. Rev.* **2016**, *116*, 3436, https://doi.org/10.1021/acs.chemrev.5b00597.

[45] M. S. Al-Keilani, N. A. Al-Sawalha, *Chem. Res. Toxicol.* **2017**, *30*, 1767, https://doi.org/10.1021/acs.chemrestox.7b00149.

[46] J. Zhu, J. A. Rodriguez-Corrales, R. Prussin, Z. Zhao, A. Dominijanni, S. L. Hopkins, B. S. J. Winkel, J. L. Robertson, K. J. Brewer, *Chem. Commun.* **2017**, *53*, 145, https://doi.org/10.1039/C6CC07978D.

[47] Z. Zhou, J. Liu, T. W. Rees, H. Wang, X. Li, H. Chao, P. J. Stang, *Proc. Natl. Acad. Sci*. **2018**, *115*, 5664, https://doi.org/10.1073/pnas.1802012115

The definitive version of this article is the electronic one that can be found at https://doi.org/10.2533/chimia.2021.845